JACS
JOURNAL OF THE AMERICAN CHEMICAL SOCIETY
Article
pubs.acs.org/JACS

# Coordination Chemistry of Disilylated Stannylenes with Group 10 $d^{10}$ Transition Metals: Silastannene vs Stannylene Complexation

Henning Arp,[†] Christoph Marschner,*[,†] Judith Baumgartner,*[,†] Patrick Zark,[‡] and Thomas Müller*[,‡]

[†]Institut für Anorganische Chemie, Technische Universität Graz, Stremayrgasse 9, 8010 Graz, Austria

[‡]Institut für Chemie, Carl von Ossietzky Universität Oldenburg, Carl von Ossietzky-Str. 9-11, 26129 Oldenburg, Federal Republic of Germany

Supporting Information

**ABSTRACT:** The coordination behavior of disilylated stannylenes toward zerovalent group 10 transition metal complexes was studied. This was accomplished by reactions of $PEt_3$ adducts of disilylated stannylenes with zerovalent group 10 transition metal complexes. The thus obtained products differed between the first row example nickel and its heavier congeners. While with nickel stannylene complex formation was observed, coordination of the stannylenes to palladium and platinum compounds led to unusual silastannene complexes of these metals. A computational model study indicated that in each case metal stannylene complexes were formed first and that the disilylstannylene/silastannene rearrangement occurs only after complexation to the group 10 metal. The isomerization is a two-step process with relatively small barriers, suggesting a thermodynamic control of product formation. In addition, the results of the computational investigation revealed a subtle balance of steric and electronic effects, which determines the relative stability of the metalastannylene complex relative to its silastannene isomer. In the case of cyclic disilylstannylenes, the Pd(0) and Pt(0) silastannene complexes are found to be more stable, while with acyclic disilylstannylenes the Ni(0) stannylene complex is formed preferentially.

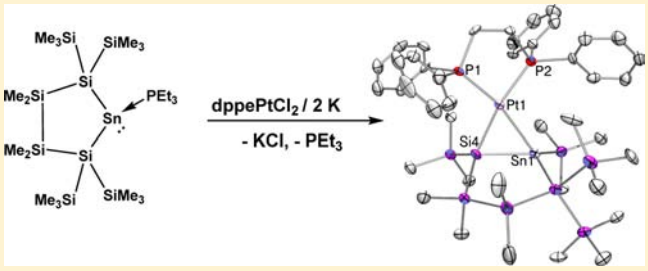


## 1. INTRODUCTION

As practically all higher tetrylenes, stannylenes are known to exhibit singlet ground states with a formal $5s^25p^2$ valence electron configuration. The vacant p-orbital is responsible for their high reactivity whereas the lone pair is inert due to its high s-character.[1] Stabilization of such compounds is frequently accomplished by attaching amino substituents, which donate electron density from their lone pair into the empty p-orbital. Stannylenes with substituents which are not $\pi$-basic are much more reactive and usually require some steric protection in order to prevent them from dimerization. Electropositive substituents to the tetrylene atom, such as alkyl or even silyl groups, diminish the singlet triplet energy gap as they enforce some hybridization of the s and p orbitals.[1] Preparation of the first bis(silyl)-substituted stannylenes was reported by Klinkhammer and co-workers some years ago.[2,3] Recently, we started some investigations concerning the chemistry of cyclic bis(silyl)-substituted germylenes,[4] stannylenes,[5] and plumbylenes.[6] Addition of the strong donor molecule $PEt_3$ allowed us to successfully trap the cyclic stannylene, which undergoes dimerization as a free species, as the respective adduct **1**.[5] This compound and the respective plumbylene adduct could be used for studying their coordination chemistry with group 4 metallocenes.[7]

The present study is now concerned with the use of **1** and a related acyclic bissilylated stannylene phosphine adduct (**9**) to investigate the coordination chemistry of silylated stannylenes as ligands for complexes of the group 10 metals in the oxidation state zero. Although dialkylstannylene complexes of palladium[8] and nickel[9] were prepared already in the early 1990s by Pörschke and co-workers, nothing is known about the coordination properties of silylated stannylenes.

## 2. RESULTS AND DISCUSSION

**Synthesis.** For the synthesis of disilylated stannylene complexes of group 4 metallocenes it proved to be a good strategy to generate the required $d^2$-metal fragment by reduction of suitable metal halides with magnesium.[7] Therefore, we decided to apply a similar approach also for group 10 metal compounds. As starting material for the preparation of platinum stannylene complexes $dppePtCl_2$ was chosen because of its ready availability and the hope that the diphenylphosphino units might provide sufficient steric protection for the anticipated stannylene ligand. Reduction of $dppePtCl_2$ with potassium in the presence of the phosphine-stabilized stannylene **1** in benzene did, however, not lead to the formation of the anticipated complex **2** (Scheme 1) as was concluded from $^{119}$Sn NMR spectroscopic data. Instead of a predicted triplet signal resulting from coupling of tin to two equivalent phosphorus atoms, the $^{119}$Sn NMR spectrum of the isolated material displayed a doublet of doublets accompanied

Received: February 15, 2013
Published: April 29, 2013

   dx.doi.org/10.1021/ja401548d | J. Am. Chem. Soc. 2013, 135, 7949−7959

**Scheme 1. Formation of Silastannene Complex 3 via the Possible Involvement of Stannylene Complex 2**

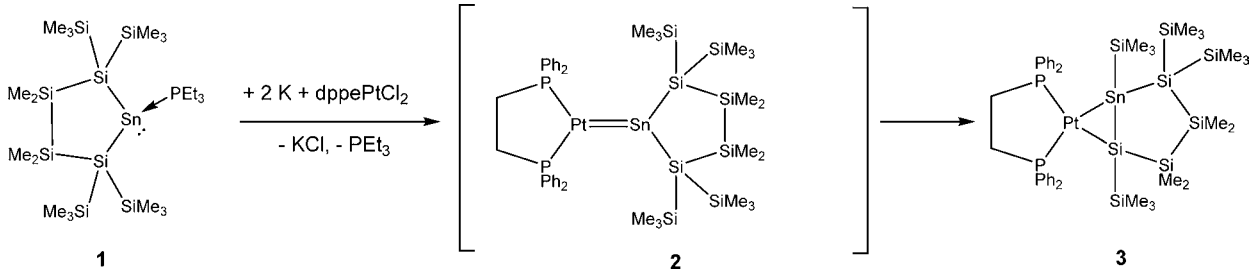


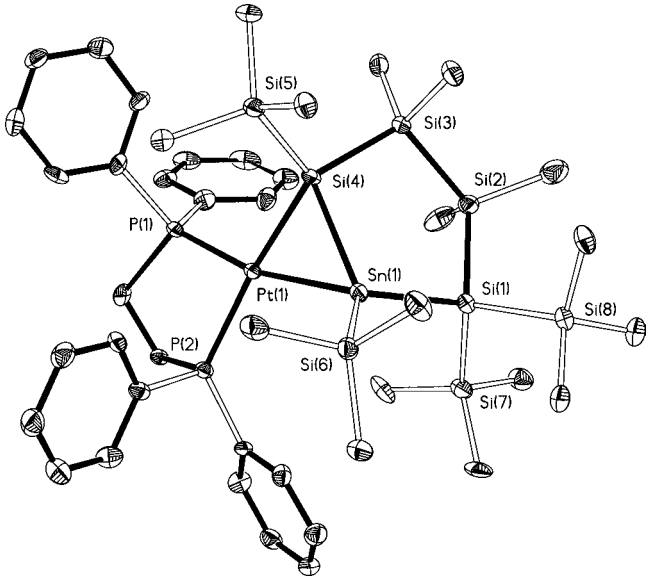


**Figure 1.** Molecular structure of **3** (thermal ellipsoid plot drawn at the 30% probability level). Hydrogen atoms omitted for clarity (bond lengths in Å, angles in deg). Sn(1)−Si(4) 2.530(3), Sn(1)−Si(6) 2.551(3), Sn(1)−Si(1) 2.577(3), Sn(1)−Pt(1) 2.6613(10), Pt(1)−P(1) 2.254(3), Pt(1)−Si(4) 2.403(3), P(1)−C(25) 1.827(12), Si(1)−Si(8) 2.330(4), Si(2)−C(2) 1.878(14), Si(4)−Sn(1)−Si(6) 122.08(11), Si(4)−Sn(1)−Si(1) 105.80(10), Si(6)−Sn(1)−Si(1) 121.35(11), Si(4)−Sn(1)−Pt(1) 55.08(7), Si(6)−Sn(1)−Pt(1) 120.99(8), Si(1)−Sn(1)−Pt(1) 113.31(8), Si(4)−Pt(1)−Sn(1) 59.69(8), Pt(1)−Si(4)−Sn(1) 65.23(8).

by $^{195}$Pt satellites. While providing evidence for direct attachment of tin to the platinum center, this pattern indicates coupling to two nonequivalent phosphorus atoms in the complex (Figure S1, Supporting Information). Accordingly, also the $^{31}$P NMR spectrum featured two doublet signals each with $^{117/119}$Sn and $^{195}$Pt satellites. Finally, the $^{29}$Si NMR spectrum showed instead of the expected three signals for a symmetric ligand eight different signals, one of them split into a doublet of doublets. From this spectroscopic behavior, the Pt complex was assumed to consist of a dppe ligand, as well as of a more complex ligand with one Si and Sn atom coordinating directly to platinum. Single crystal X-ray crystallographic analysis showed this assumption to be correct and the compound to be the platinum silastannene complex **3** (Figure 1, Scheme 1).

In rearrangement and redistribution reactions of oligosilanyl transition metal complexes silyl−silylene complexes were proven to be essential intermediates.[10−13] 1,2-Silyl shift reactions allow oligosilanyl transition metal complexes avoiding coordinative unsaturation, which may occur in the event of ligand dissociation. Mechanistically the formation of **3**, was thought to involve stannylene complex **2** as an intermediate. Subsequent migration of a $SiMe_3$ group from one of the quaternary silicon atoms to the adjacent tin center would then effect the conversion to **3**.

After this unexpected result we decided to investigate the coordination behavior of silylated stannylenes toward palladium by reacting **1** with $Pd(PPh_3)_4$. This precursor complex was used to exclude a possible involvement of elemental potassium in the rearrangement reaction. NMR spectroscopic analysis of the reaction mixture in benzene showed a very similar coupling pattern as was found for **3** and thus proved the formation of the mixed phosphine palladium silastannene complex **4** (Scheme 2) which however could not be isolated in pure form. The reaction was therefore repeated using $Pd(PEt_3)_4$ as the transition metal starting material and proceeded smoothly to yield bis-

**Scheme 2. Synthesis of dppe Palladium Silastannene Complex 6**

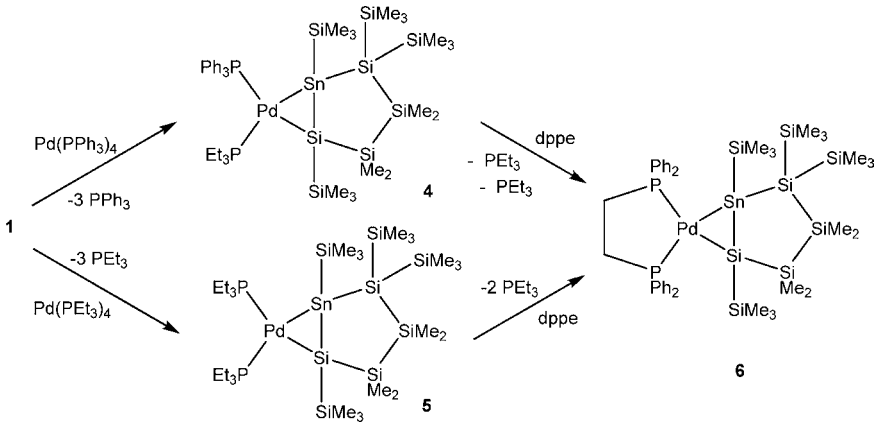



dx.doi.org/10.1021/ja401548d | J. Am. Chem. Soc. 2013, 135, 7949−7959

(triethylphosphine) palladium silastannene complex **5**, but again isolation of the material in crystalline form failed due to its very high solubility. Finally, from both reaction mixtures the identical complex **6** could be obtained and isolated by addition of 1 equiv dppe (Scheme 2). After recrystallization from pentane, crystals of **6** suitable for X-ray diffraction analysis were obtained (Figure 2).

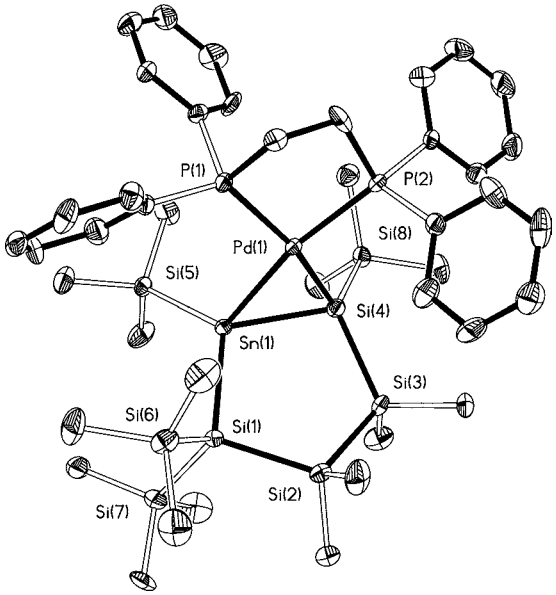


**Figure 2.** Molecular structure of **6** (thermal ellipsoid plot drawn at the 30% probability level). Hydrogen atoms omitted for clarity (bond lengths in Å, angles in deg). Pd(1)−P(2) 2.307(3), Pd(1)−Si(4) 2.411(3), Pd(1)−Sn(1) 2.6714(12), Sn(1)−Si(4) 2.503(3), Sn(1)−Si(5) 2.570(3), Sn(1)−Si(1) 2.586(3), P(1)−C(19) 1.838(10), Si(1)−Si(7) 2.322(4), Si(5)−C(6) 1.860(11), Si(4)−Pd(1)−Sn(1) 58.75(7), Si(4)−Sn(1)−Si(5) 122.90(10), Si(4)−Sn(1)−Pd(1) 55.42(7), Pd(1)−Si(4)−Sn(1) 65.84(7).

To test whether this silyl migration behavior is an intrinsic property of the cyclic nature of the oligosilanylene substituent attached to tin, we decided to utilize Klinkhammer's procedure for the preparation of the acyclic bis[tris(trimethylsilyl)silyl]-stannylene[2] to prepare the triethylphosphine adduct **9**. Formation of an analogous trimethylphosphine stannylene adduct was mentioned by Klinkhammer without providing any preparative or characterization details.[3] Recently, Castel and co-workers also published an NHC stabilized version of this particular stannylene.[14] Our attempts to adapt Klinkhammer's procedure for the synthesis of bis[tris(trimethylsilyl)silyl]-stannylene led, however, to the formation of the stannylene potassium amide adduct **7** (Scheme 3). This failure was likely caused by using an alternative reaction for the synthesis of tris(trimethylsilyl)silylpotassium[15] and our inability to properly remove THF[16] from the silanide after the initial reaction of tetrakis(trimethylsilyl)silane and *t*BuOK in THF.[17] The thus partly soluble potassium bis(trimethylsilyl)amide led to the formation of **7**. In a similar way also the amide adduct of the cyclic stannylene is accessible.[5] Synthesis of the desired stannylene phosphine adduct **9** was eventually accomplished by salt metathesis reaction between tris(trimethylsilyl)-silylpotassium and the triethylphosphine adduct of $SnCl_2$[18] (**8**) (Scheme 4).

**Scheme 3. Formation of Bis[tris(trimethylsilyl)silyl]stannylene Amide Adduct 7**

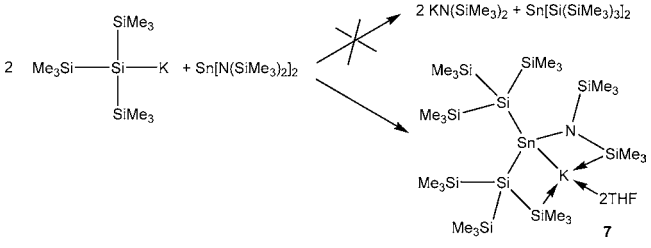


**Scheme 4. Formation of Bis[tris(trimethylsilyl)silyl]tin Triethylphosphine Adduct 9 and Silastannene Palladium Complex 10**

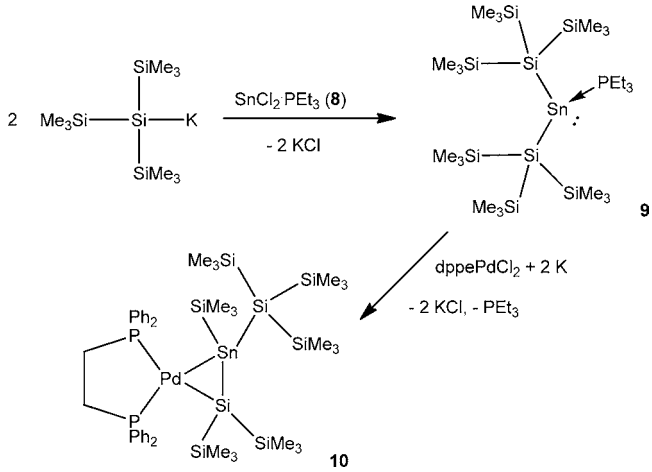


Complex **9** was treated with potassium and $dppePdCl_2$ to form silastannene palladium complex **10** with an acyclic silastannene unit again formed by migration of a trimethylsilyl group from one of the tris(trimethylsilyl)silyl fragments to the tin atom (Scheme 4).

A different reactivity pattern was observed for the coordination of **9** to a nickel complex. When **9** was reacted with $Ni(COD)_2$[19] and an additional equivalent of $PEt_3$ instead of a nickel silastannene complex the initially anticipated stannylene complex **11** was isolated (Scheme 5). This observation is in line with Kira's[20] recent synthesis of a nickel silylene complex and older work by Pörschke[9] yielding dialkylstannylene nickel complexes. Complex **11** exhibits the expected NMR spectroscopic properties for stannylene complexes.

**Scheme 5. Formation of Nickel Stannylene Complex 11**

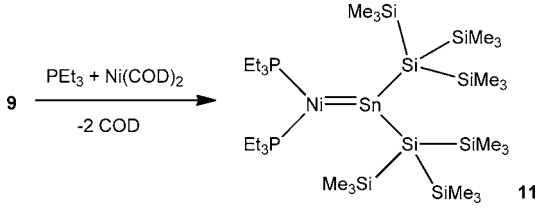


**NMR Spectroscopy.** Multinuclear NMR spectroscopy is probably the most useful tool to get insight into the bonding situation of the studied transition metal silastannene and stannylene complexes. $^{119}Sn$ NMR spectra are particularly


dx.doi.org/10.1021/ja401548d | J. Am. Chem. Soc. 2013, 135, 7949−7959

diagnostic. While the typical region for the chemical shift of doubly bonded tin atoms is downfield of +400 ppm, the $^{119}$Sn NMR resonances of **3**, **4**, **5**, **6**, and **10** were found to exhibit shifts of $\delta$ = −488.0 ppm, −280.3 ppm, −310.2 ppm, −316.3 ppm, and −430.2 ppm, respectively. A comparison with the $^{119}$Sn shift of [(dmpe)Pd(SnPh$_3$)$_2$][21] of −40.4 ppm suggests metallacycle stannyl−Pt/Pd type bonds with the resonances shifted further upfield because of the silyl substituents and the three-membered ring. In a similar way, also the $^{29}$Si NMR shifts of the metal bound silicon atom can be interpreted. For a palladium $\pi$-complex of a tetrasilylated disilene Kira and co-workers observed a $^{29}$Si NMR resonance at $\delta$ = 65 ppm,[22] while for the metallacycle derivatives of the same disilene shifts close to $\delta$ = −50 ppm[23,24] were recorded. The latter values compare well to the silastannene complexes **3**, **4**, **5**, **6**, and **10** with chemical shifts of $\delta$ = −62.5 ppm, −35.8 ppm, −42.2 ppm, −30.8 ppm, and −40.8 ppm, respectively. The most pronounced upfield shifts of **3** suggests that the $\pi$-back bonding from the transition metal to the silastannene unit is stronger in the Pt complexes than in the Pd analogues in accordance with earlier observations on disilene complexes.[25]

The presence of four spin $^1/_2$ heteronuclei in the case of **3**, and three of these nuclei for **4**, **5**, **6**, and **10** involved in the silastannene complexes allows a very good NMR-spectroscopic description of these compounds. In all cases couplings of the coordinated Sn and Si atoms with *cis*- and *trans*- located P atoms were observed. The strong degree of asymmetry induced by the 1,2-silyl shift and the coordination to the metal is reflected in the $^1$H, $^{13}$C, and $^{29}$Si spectra of **3**, **4**, **5**, and **6**. The respective stannylene complexes would exhibit only one resonance each for the trimethylsilyl groups, the dimethylsilylene units, and the quaternary silicon atoms. For the silastannene-complexes the symmetry of the left and right side and of the top and bottom side of the five-membered ring is broken. Therefore, four different signals for the trimethylsilyl groups were found in the $^1$H, $^{13}$C, and $^{29}$Si spectra. Conversely, four signals were observed for the methyl groups of the SiMe$_2$ units in the $^1$H and $^{13}$C spectra.

The same asymmetry also transfers to the signals of the phosphine ligand. The two nonequivalent phosphorus atoms give rise to two doublets of doublets in the $^{31}$P spectra. In addition satellites from the coupling to $^{117/119}$Sn and for **3** to $^{195}$Pt can be observed. The $^{31}$P resonances of the dppe ligand were found at 61.1 and 42.6 ppm for **3** and at 40.4 and 23.5 ppm for **6** with $^2J$(PP) couplings of 10 and 13 Hz, respectively. Although the *trans*- and *cis*-$^2J$(PSn) couplings of the silastannene complexes are quite different, the magnitude of this difference is much smaller than reported for complexes of the type: (R$_3$P)$_2$M(X)SnR′$_3$ (*M* = Pt, Pd; X = halide, alkyl, aryl).[26,27] For compounds **3** and **6**, bearing the dppe ligands; *trans*-$^2J$(PSn) couplings of 668 (**3**) and 560 (**6**) Hz were observed, while the *cis*-$^2J$(PSn) coupling constants for both were close to 110 Hz. Complexes **4** and **5** with nonchelating phosphine ligands exhibited *trans*-$^2J$(PSn) couplings of 641 (**4**) and 656 (**5**) Hz and the *cis*-$^2J$(PSn) couplings for both amounted to 161 Hz. On the other hand was the $^1J$(PtSn) coupling constant of **3** of 2990 Hz found to be unexpectedly large.[26,27] A similar coupling pattern as observed for the $^2J$(PSn) couplings was also detected in the $^{29}$Si NMR spectra. Larger *trans*- than and *cis*-$^2J$(PSi) couplings lay in the ranges from 91 to 102 Hz for the *trans*- and from 14 to 26 Hz for the *cis*-$^2J$(PSi) couplings for compounds **3**−**6**.

The $^{31}$P NMR spectroscopic properties of the Pd-silastannene complex **10** are comparable to that of **6**. Chemical shifts of 40.8 and 26.0 ppm are almost identical and also the $^2J$(PP) of 10 Hz is similar. Only the *trans*- and *cis*-$^2J$(PSn) couplings of 635 and 89 Hz indicate that these values change when the Pd-attached stannyl group is not part of a cyclic system. *Trans*- and *cis*-$^2J$(PSi) couplings of **10** were detected as 89 and 16 Hz, respectively .

In contrast to all other complexes reported, the $^{119}$Sn NMR spectrum of **11** showed a triplet with a typical stannylene chemical shift of $\delta$ 1314 ppm and a $^2J$(SnP) coupling constant of 611 Hz. The $^{29}$Si NMR spectrum consisted of the expected two signals found in typical regions (−10.1 ppm for SiMe$_3$ and −94.0 ppm for the quaternary Si).

**X-ray Crystallography.** Compounds **3**, **6**, **7**, **8**, **9**, **10**, and **11** were subjected to single-crystal X-ray diffraction analysis, and the crystallographic details are listed in Tables S1 and S2, Supporting Information. For the structurally characterized silastannene transition metal complexes **3** (Figure 1), **6** (Figure 2), and **10** (Figure 6) the Sn − Si bonding distances of the formal double bonds lie with 2.52 Å (**3**), 2.50 Å (**6**), and 2.52 Å (**10**) in between the values for a Si═Sn double bond in Sekiguchi's[28] free silastannene Tip$_2$Sn═Si(Si*t*Bu$_2$Me)$_2$ (2.42 Å) and an ordinary Sn−Si single bond (2.60 Å).[29] The Pd−Si distances of 2.41 Å (**6**) and 2.42 Å (**10**) are in accordance with Kira's palladium disilene complexes.[24] The Pt or Pd atoms show a distorted square planar coordination geometry. The angles between the P$_2$M and SnSiM planes (M = Pt, Pd) were found to be about 30° each. These structural parameters indicate that the silastannene complexes are best described as metallacycles. The obtained crystal structure of the stannylene amide adduct **7** (Figure 3) shows rather long Si−Sn bond distances of 2.71 Å and 2.75 Å (Figure 3), but compares well to Klinkhammer's K[(Me$_3$Si)$_3$SnKSn(SiMe$_3$)$_3$] with a Si−Sn

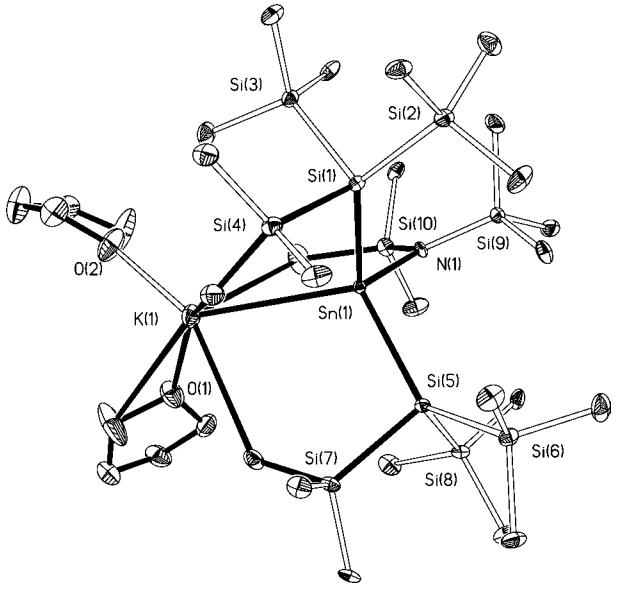


**Figure 3.** Molecular structure of **7** (thermal ellipsoid plot drawn at the 30% probability level). Hydrogen atoms omitted for clarity (bond lengths in Å, angles in deg). Sn(1)−N(1) 2.164(6), Sn(1)−Si(1) 2.713(2), Sn(1)−Si(5) 2.752(2), Sn(1)−K(1) 3.557(2), N(1)−Si(9) 1.725(6), Si(1)−Si(4) 2.358(3), Si(2)−C(1) 1.871(9), Si(1)−Sn(1)−Si(5) 112.77(7), N(1)−Sn(1)−K(1) 118.02(16), Si(1)−Sn(1)−K(1) 104.46(6), Si(5)−Sn(1)−K(1) 110.93(6).


dx.doi.org/10.1021/ja401548d | *J. Am. Chem. Soc.* 2013, 135, 7949−7959

bond lengths of 2.73 Å.[30] Also for the starting material $SnCl_2 \cdot PEt_3$ (**8**) the crystal structure was obtained (Figure 4). Its

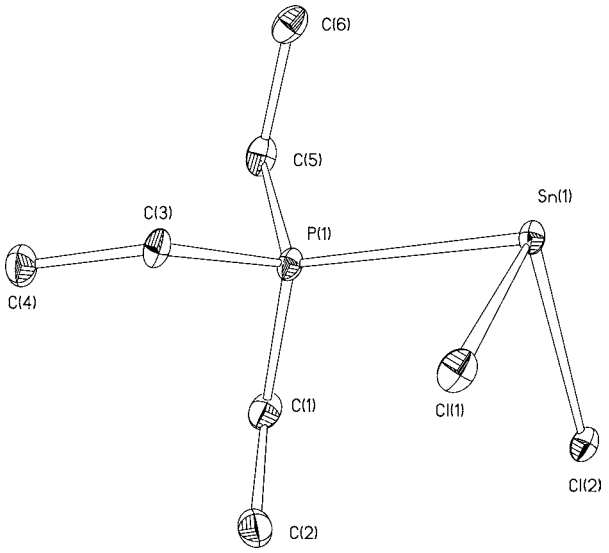


**Figure 4.** Molecular structure of **8** (thermal ellipsoid plot drawn at the 30% probability level). Hydrogen atoms omitted for clarity (bond lengths in Å, angles in deg). Sn(1)−Cl(1) 2.5182(15), Sn(1)−Cl(2) 2.5322(15), Sn(1)−P(1) 2.7032(16), P(1)−C(5) 1.822(6), Cl(1)−Sn(1)−Cl(2) 90.86(5), Cl(1)−Sn(1)−P(1) 87.00(5), Cl(2)−Sn(1)−P(1) 88.98(5).

Sn − P bond length of 2.70 Å is significantly longer than the 2.61 Å found in **1**.[5] Most noteworthy are the bond angles around tin as they are all very close to 90°, thus indicating a strong inert pair effect of the remaining electron pair in the 5s orbital. The structure of **9** (Figure 5) shows the expected similarities to **1**.[5] The donor−acceptor interaction with the phosphine is indicated by the strong pyramidalization of the Sn atom in **9** [pyramidalization angle $\beta$(Sn) = 78.4°][31] and by the length of the Sn−P bond (2.65 Å). In the crystal structure of **11** (Figure 7), a short Ni═Sn distance of 2.42 Å is found (close to 2.39 Å reported for other Ni−Sn double bonds)[9] and the PNiP plane and the SiSnSi plane are perpendicular to each other. The spectroscopic and crystallographic observations clearly thus indicate a high contribution of $\pi$-back bonding to the Sn−Ni interaction.

**Computational Results.** Quantum mechanical computations applying the M06−2X density functional were used[32] to gain insight into the factors that are responsible for the formation of the silastannenes complexes **3** - **6**, and **10** from palladium and platinum precursor compounds and for the preference of the stannylene nickel complex **11** over its silastannene isomer. Previously, we found that stannylene **12**, *in situ* generated from complex **1** by reaction with Lewis acids, dimerizes to the endocyclic distannene **13**. As a reasonable intermediate the exocyclic distannene **14** was assumed (Scheme 6).[5] In this earlier study, no products arising from an isomeric silastannene **15** were detected. This is in perfect agreement with the results from the present density functional study which predict that silastannene **15** is significantly less stable than stannylene **12** ($\Delta G^{(298)}$ = 44 kJ mol$^{-1}$). In addition a substantial activation barrier ($\Delta G^{\ddagger(298)}$ = 106 kJ mol$^{-1}$) separates both isomers. These computational results suggest that at ambient temperature the formation of silastannene **15** from stannylene **12** at detectable rates can be securely excluded (Scheme 6). On the other hand, these computational results clearly indicate that the silyl group migration, which is required for the formation of

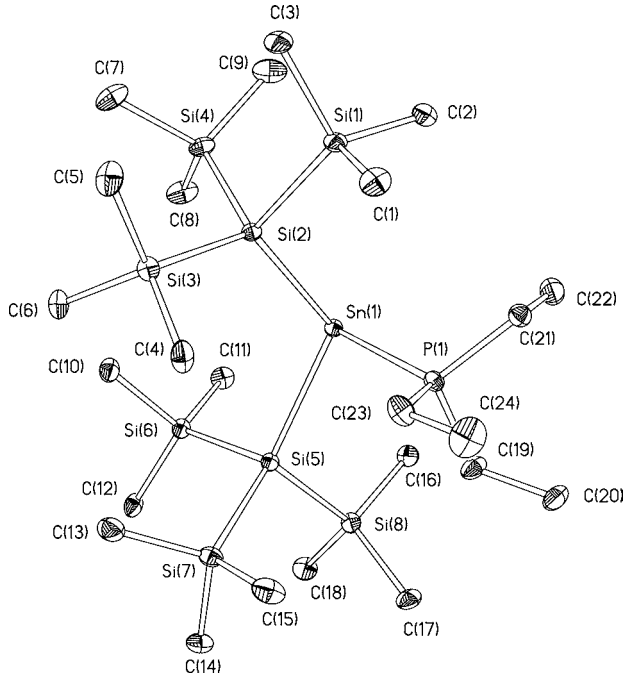


**Figure 5.** Molecular structure of **9** (thermal ellipsoid plot drawn at the 30% probability level). Hydrogen atoms omitted for clarity (bond lengths in Å, angles in deg). Sn(1)−P(1) 2.6477(14), Sn(1)−Si(2) 2.6936(13), Sn(1)−Si(5) 2.7165(14), P(1)−C(19) 1.830(5), Si(1)−C(1) 1.896(5), Si(1)−Si(2) 2.3651(19), P(1)−Sn(1)−Si(2) 97.92(4), P(1)−Sn(1)−Si(5) 94.40(4), Si(2)−Sn(1)−Si(5) 114.21(4), Si(3)−Si(2)−Sn(1) 125.83(6), Si(1)−Si(2)−Sn(1) 111.03(6), Si(4)−Si(2)−Sn(1) 103.68(6).

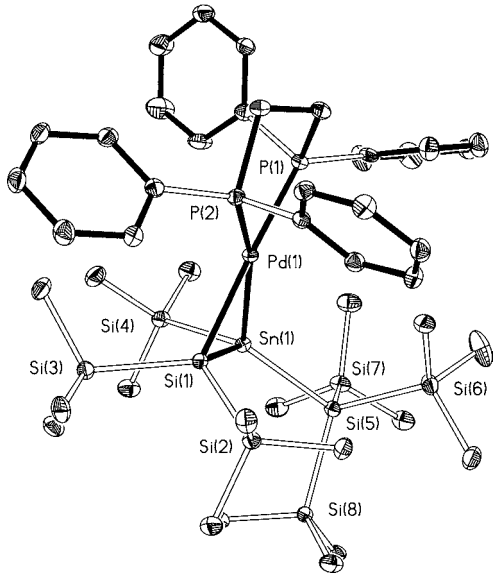


**Figure 6.** Molecular structure of **10** (thermal ellipsoid plot drawn at the 30% probability level). Hydrogen atoms omitted for clarity (bond lengths in Å, angles in deg). Sn(1)−Si(1) 2.5177(12), Sn(1)−Si(4) 2.5872(13), Sn(1)−Si(5) 2.6042(13), Sn(1)−Pd(1) 2.6808(6), Pd(1)−P(2) 2.3048(11), Pd(1)−Si(1) 2.4211(12), P(1)−C(27) 1.830(4), Si(1)−Si(2) 2.3406(17), Si(2)−C(1) 1.874(4), Si(4)−Sn(1)−Si(5) 114.69(4), Si(1)−Sn(1)−Pd(1) 55.41(3), Si(1)−Pd(1)−Sn(1) 58.88(3), Pd(1)−Si(1)−Sn(1) 65.71(3).


dx.doi.org/10.1021/ja401548d | J. Am. Chem. Soc. 2013, 135, 7949−7959

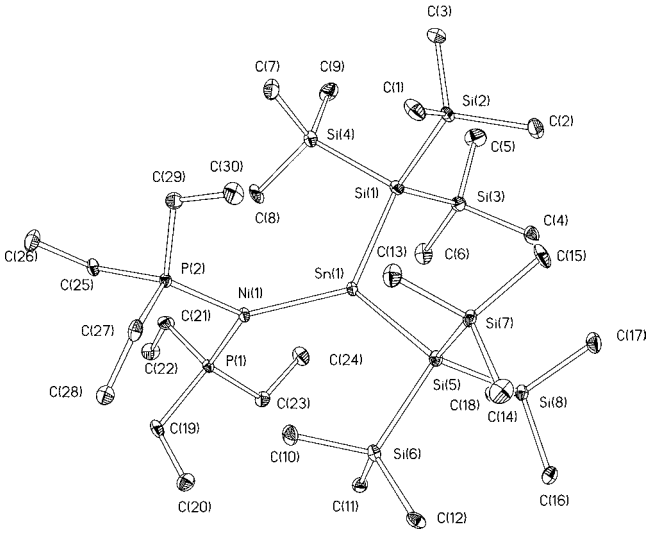


**Figure 7.** Molecular structure of **11** (thermal ellipsoid plot drawn at the 30% probability level). Hydrogen atoms omitted for clarity (bond lengths in Å, angles in deg). Ni(1)−P(1) 2.2043(18), Ni(1)−Sn(1) 2.4177(10), Sn(1)−Si(5) 2.6468(19), Sn(1)−Si(1) 2.6468(19), P(1)−C(19) 1.841(7), Si(1)−Si(3) 2.352(3), Si(2)−C(3) 1.878(7), P(2)−Ni(1)−P(1) 109.21(7), P(2)−Ni(1)−Sn(1) 123.64(5), P(1)−Ni(1)−Sn(1) 127.00(5), Ni(1)−Sn(1)−Si(5) 123.64(5), Ni(1)−Sn(1)−Si(1) 121.73(5), Si(5)−Sn(1)−Si(1) 114.46(6).

the silastannene complexes **3**–**6**, and **10** occurs in the coordination sphere of the $d^{10}$ metal.

The reactivity of the stannylene phosphine complex **1** is clearly dominated by its high lying lone pair at the tin atom. It is therefore reasonable to assume that compound **1** acts initially as a simple two electron donor versus the *in situ*-generated $14e^-$ $d^{10}ML_2$ complex (*M* = Ni, Pd, Pt, $L_2$ = dppe, depe). Consequently, the formation of complexes **16** with tetracoordinated tin atoms and tricoordinated M-atoms is the logical starting point for the computational study (Scheme 7). The first question to be addressed by the computations is, whether the removal of the $PEt_3$ ligand from the tin atom and formation of the metal stannylene complexes **17** is thermodynamically a viable reaction course (Scheme 7). Clearly connected with this question is the relative stability of the $18e^-$ metal complexes **18** which can be formed either intra- or intermolecularly from compounds **16**. In this computational study, we initially used the dimethylphosphinoethylene (dmpe)-ligand instead of its diphenyl (dppe) or diethyl (depe) derivatives to complete the coordination sphere of the $d^{10}$ metal in order to minimize computational costs. These model compounds are labeled with the superscript Me to indicate the use of the dmpe ligand.

The computed bond dissociation energy (BDE) for the Sn−P bond in complex $\mathbf{16}^{Me}$ is for all three stannyl metal complexes relatively small ($\mathbf{16a}^{Me}$ (M = Ni): 44 kJ $mol^{-1}$; $\mathbf{16b}^{Me}$ (M = Pd): 63 kJ $mol^{-1}$; $\mathbf{16c}^{Me}$ (M = Pt): 54 kJ $mol^{-1}$, see Scheme 7, Figure 8 and Table S3 in the Supporting Information). In consequence, the inclusion of thermal contributions and entropy effects results in negative free Gibbs energies at 298 K for the dissociation reaction $\mathbf{16}^{Me} \rightarrow \mathbf{17}^{Me} + PEt_3$ (Figure 8). In addition, the results of the computations suggest that for all three metals the $18e^-$ complex $\mathbf{18}^{Me}$ is less stable than the $16e^-$ species $\mathbf{16}^{Me}$ (Figure 8). Therefore, it is indicated that $d^{10}$ metal stannylene complexes **17** are the primary reaction products formed when precursors for $d^{10}ML_2$ complexes are brought to reaction with stannylene phosphine complex **1**.

In the framework of our computations using metal stannylenes $\mathbf{17}^{Me}$ as close models, we were not able to identify a reaction sequence that transforms the compounds $\mathbf{17}^{Me}$ in one single step into the silastannene complexes $\mathbf{19}^{Me}$. In detail, we did not accomplish to locate transition state structures which allow for the most evident reaction mechanism: a 1,2 silyl shift from the $\alpha$-silicon atom to the tin atom in compound $\mathbf{17}^{Me}$ with an accompanying change of the topology of the molecule to form the metallacyclopropane structure in complexes $\mathbf{19}^{Me}$. Instead, the results of our computations predict a two-step mechanism via cyclic metallostannylene intermediates $\mathbf{20}^{Me}$ with M-Sn(II)-Si linkage (Scheme 8).[33−40] The calculated structures for all stationary points along the

**Scheme 6. Intermediate Formation of Stannylene 12 and its Possible Follow up Chemistry[5]**

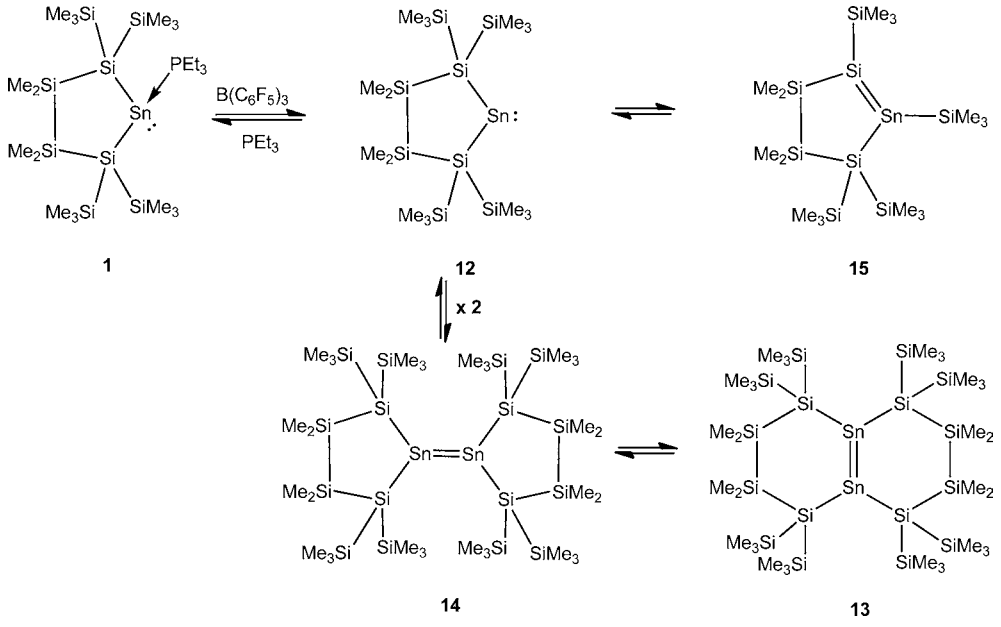



dx.doi.org/10.1021/ja401548d | J. Am. Chem. Soc. 2013, 135, 7949−7959

**Scheme 7. Formation of Stannylene Complexes 17 (a: M = Ni, b: M = Pd, c: M = Pt; $L_2$ = dmpe)**

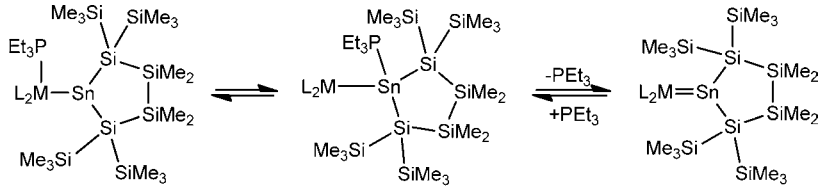


18 16 17

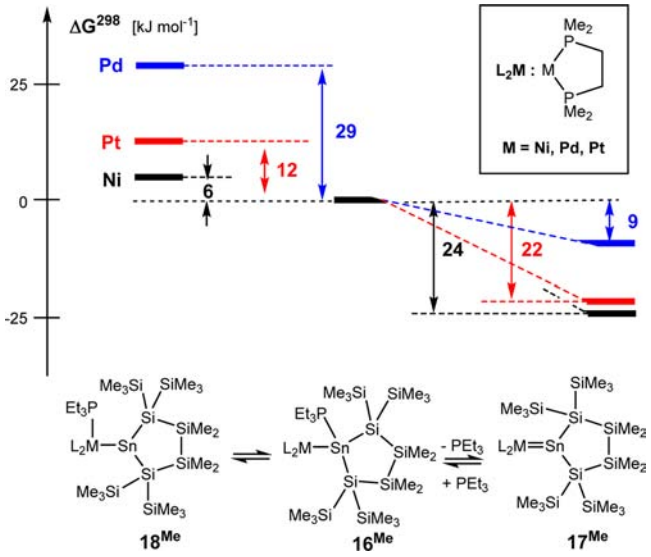


**Figure 8.** Thermodynamic relations between the $d^{10}$-metal complexes $\mathbf{16}^{Me}$, $\mathbf{18}^{Me}$ and $\mathbf{17}^{Me}$ + $PEt_3$. Calculated at M06–2X/6-31G(d) (P,Si,C,H), def2-tzvp (Sn,Ni,Pd,Pt). Free Gibbs energy differences $\Delta G^{298}$ are given relative to $G^{298}$ of compounds $\mathbf{16}^{Me}$. Values for the Ni species $\mathbf{16a}^{Me}$–$\mathbf{18a}^{Me}$ are given in black, those for Pd compounds $\mathbf{16b}^{Me}$–$\mathbf{18b}^{Me}$ are given in blue and those for Pt compounds $\mathbf{16c}^{Me}$–$\mathbf{18c}^{Me}$ are given in red.

isomerization reaction $\mathbf{17b}^{Me} \rightarrow \mathbf{19b}^{Me}$ of the palladium–tin complexes are given in Figure 9. The metallostannylene species $\mathbf{20}^{Me}$ are formed by 1,2-silyl group migrations from the tin to the $d^{10}$ metal atom with accompanying ring expansion. Subsequent 1,3-silyl group migrations from the $\alpha$-silicon atoms to the tin atoms are followed by bond formations between the $\alpha$-silicon and tin atoms and yield the silastannene complexes $\mathbf{19}^{Me}$ (Scheme 8).

The computations reveal the somehow surprising results that for each metal the silastannene complexes $\mathbf{19}^{Me}$ are more stable than the corresponding stannylene isomers $\mathbf{17}^{Me}$ (Figure 10). This is not an artifact of the used model system; the relative sequence in energy was also found for the respective isomeric dppe-complexes. In that case, the silastannene complexes **3**, **6**, **19** are more stable by −15 kJ $mol^{-1}$ (**19a**, M = Ni), by −19 kJ $mol^{-1}$ (**6**, M = Pd) and by −36 kJ $mol^{-1}$ (**3**, M = Pt) compared to the corresponding metal-stannylenes **17a** (M = Ni), **17b** (M = Pd), **17c** (M = Pt) (see Table S3, in the Supporting Information). These results are in agreement with the isolation of the palladium and platinum compounds **6** and **3**. They provide, however, no rationale for the obvious stability of nickel stannylene complex **11** versus this two-step rearrangement. At this point it is of interest to note that our computations use as models cyclic disilylstannylenes, while the isolated nickel stannylene complex **11** results from the reaction of the acyclic bis[tris(trimethylsilyl)silyl]stannylene phosphine complex **9**. Calculations for the experimentally investigated compounds show that in this case the nickel-stannylene complex **11** and the silastannene isomer **21** are nearly identical in energy. In fact, at $T$ = 298 K the stannylene complex **11** is even thermodynamically slightly favored compared to its silastannene isomer **21** ($\Delta G^{298}$ = −15 kJ $mol^{-1}$). A closer inspection of the computed reaction coordinates for the metal-stannylene/metal-silastannene rearrangements $\mathbf{17}^{Me} \rightarrow \mathbf{19}^{Me}$ shows that the intermediates $\mathbf{20}^{Me}$ are for all three metals separated by only small barriers either from the product $\mathbf{19}^{Me}$ (in the case of $M$ = Pt, $\Delta G^{‡}$ = 13 kJ $mol^{-1}$) or from the starting material $\mathbf{17}^{Me}$ (in the case of M = Ni, $\Delta G^{‡}$ = 15 kJ $mol^{-1}$ and M = Pd, $\Delta G^{‡}$ = 19 kJ $mol^{-1}$). Therefore, it is reasonable to assume that intermediates such as $\mathbf{20}^{Me}$ cannot be detected at ambient

**Scheme 8. Mechanistic Rationale for the Formation of Silastannene Complexes 3, 6, 19 from Stannylene Complexes 17**

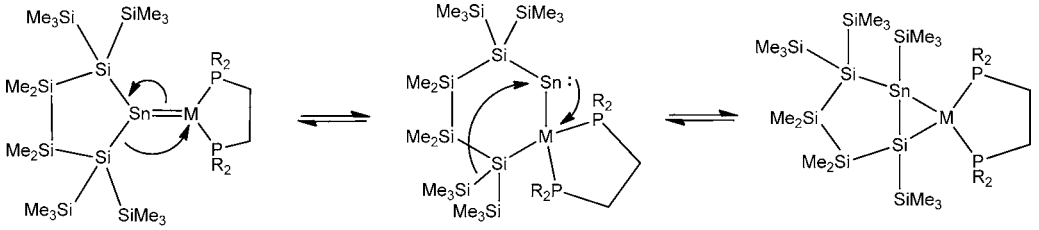


R = Me : $\mathbf{17a}^{Me}$: M = Ni; $\mathbf{17b}^{Me}$: M = Pd; $\mathbf{17c}^{Me}$: M = Pt

R = Ph : **17a**: M = Ni; **17b**: M = Pd; **17c**: M = Pt

R = Me : $\mathbf{20a}^{Me}$: M = Ni; $\mathbf{20b}^{Me}$: M = Pd; $\mathbf{20c}^{Me}$: M = Pt

R = Ph : **20a**: M = Ni; **20b**: M = Pd; **20c**: M = Pt

R = Me : $\mathbf{19a}^{Me}$: M = Ni; $\mathbf{19b}^{Me}$: M = Pd; $\mathbf{19c}^{Me}$: M = Pt

R = Ph : **19a**: M = Ni; **6**: M = Pd; **3**: M = Pt


dx.doi.org/10.1021/ja401548d | J. Am. Chem. Soc. 2013, 135, 7949–7959

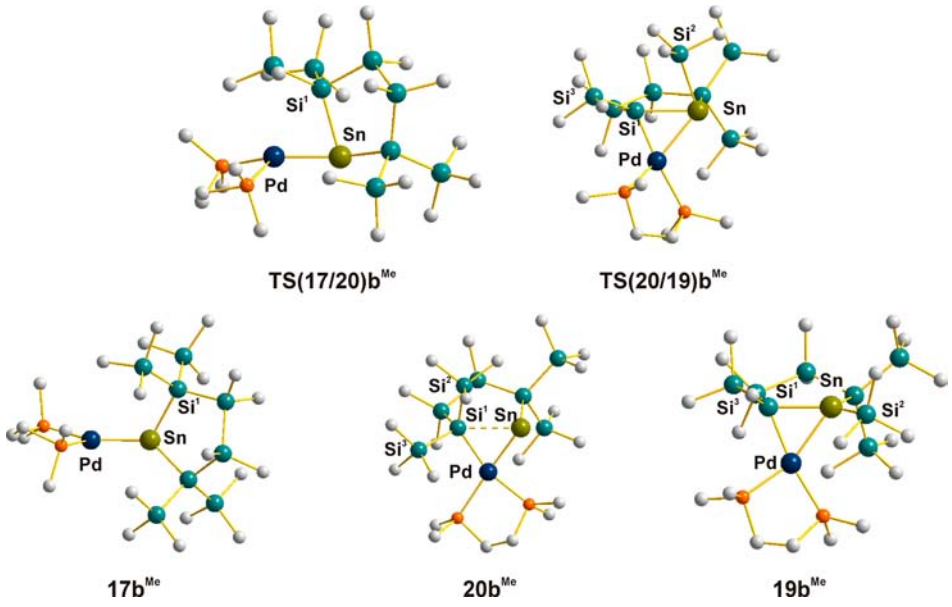


**Figure 9.** Calculated molecular structures of palladium tin complexes **17b**$^{Me}$, **20b**$^{Me}$, **19b**$^{Me}$ and transition states connecting them (at M06−2X/def2-tzvp(Pd,Sn),6-31G(d)(P, Si, C, H); all hydrogen atoms are omitted. Color code: Sn, olive; Pd, dark blue; P, orange; Si, teal; C, light gray). Pertinent calculated structural parameter (atomic distances are given in [pm], bond angles and dihedral angles in deg: **17b**$^{Me}$: Pd − Sn = 255.9, Sn − Si$^1$ = 263.8, Pd − Sn − Si$^1$ = 119.3; **TS(17b/20)b**$^{Me}$: Pd − Sn = 256.5, Sn − Si$^1$ = 273.6, Pd − Si$^1$ = 321.3, Pd − Sn − Si$^1$ = 75.5; **20b**$^{Me}$: Pd − Sn = 261.8, Sn − Si$^1$ = 287.6, Pd − Si$^1$ = 251.8, Si$^1$ − Si$^2$ = 239.6, Sn − Si$^2$ = 344.3, Si$^3$ − Si$^1$ − Sn$^1$ − Si$^2$ = −93.3; **TS(20/19)b**$^{Me}$: Pd − Sn = 278.1, Sn − Si$^1$ = 267.1, Pd − Si$^1$ = 234.6, Si$^1$ − Si$^2$ = 317.6, Sn − Si$^2$ = 266.5, Si$^3$ − Si$^1$ − Sn$^1$ − Si$^2$ = −48.9; **19b**$^{Me}$: Pd − Sn = 273.0, Sn − Si$^1$ = 248.3, Pd − Si$^1$ = 240.1, Si$^1$ − Si$^3$ = 232.4, Sn − Si$^2$ = 256.5, Si$^3$ − Si$^1$ − Sn$^1$ − Si$^2$ = 34.8.

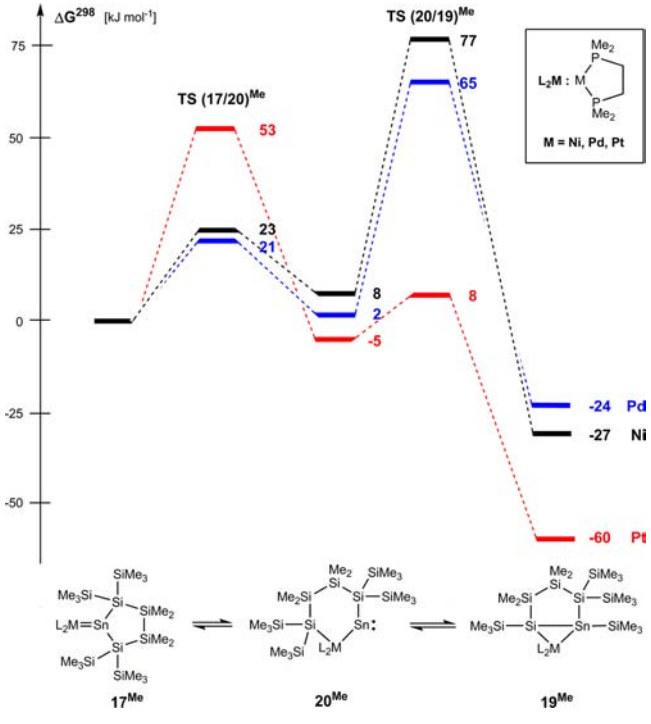


**Figure 10.** Calculated reaction paths for the rearrangement of stannylene complexes **17**$^{Me}$ to give silastannene complexes **19**$^{Me}$ via the intermediate **20**$^{Me}$. Calculated at M06−2X/6-31G(d) (P, Si, C, H), def2-tzvp (Sn, Ni, Pd, Pt). Free Gibbs energy differences $\Delta G^{298}$ are given relative to $G^{298}$ of compounds **17**$^{Me}$. Values for the Ni species **17a**$^{Me}$, **19a**$^{Me}$ and **20a**$^{Me}$ are given in black, those for Pd compounds **17b**$^{Me}$, **19b**$^{Me}$ and **20b**$^{Me}$ are given in blue and those for Pt compounds **17c**$^{Me}$, **19c**$^{Me}$ and **20c**$^{Me}$ are given in red.

conditions during the rearrangements. For the platinum compounds, the first step, the formation of the intermediate **20c**$^{Me}$, is connected with the highest barrier. In the cases of nickel and palladium, it is the product forming process to give either **19a**$^{Me}$ or **19b**$^{Me}$ which is rate-determining (Figure 10). The calculated overall barriers for the metal-stannylene/metal-silastannene rearrangements **17**$^{Me}$ → **19**$^{Me}$ for the different group 10 metals are clearly hierarchized, with the highest barrier predicted for the nickel system (77 kJ mol$^{-1}$ for **TS(20a/19a)**$^{Me}$ vs 65 kJ mol$^{-1}$ for **TS(20b/19b)**$^{Me}$ (Pd) and 53 kJ mol$^{-1}$ for **TS(17c/20c)**$^{Me}$ (Pt)). This result suggests that the stability of nickel-stannylene complexes, such as **11**, is also connected with the higher barrier for the rearrangement to the nickel-silastannene isomer and therefore kinetic factors are of importance.

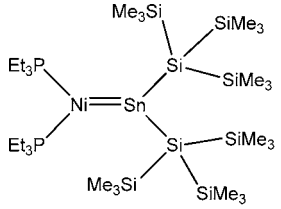


**11**

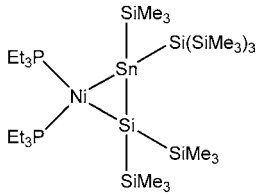


**21**

## 3. CONCLUSION

In the course of investigating the chemistry of bissilylated tetrylenes the current study describes reactions of phosphine adducts of bissilylated stannylenes (**1**,**9**) with zerovalent diphosphine complexes of platinum, palladium, and nickel. Surprisingly, reactions with Pt(0) and Pd(0) complexes did not yield the respective stannylene complexes but rather silastannene complexes (**3**, **4**, **5**, **6**, **10**) where the coordinated


dx.doi.org/10.1021/ja401548d | J. Am. Chem. Soc. 2013, 135, 7949−7959

unit is the product of a 1,2-trimethylsilyl shift of the stannylene to the Sn atom. This behavior was observed for a cyclic (**1**) and an acyclic (**9**) stannylene $PEt_3$ adduct. A similar attempt to react the acyclic stannylene adduct with a Ni(0) precursor compound led to the expected Ni-stannylene complex (**11**). The results of a computational investigation for the reaction of the cyclic bisilylated stannylene phosphine complex **1** with $d^{10}$ M dmpe complexes (M = Ni, Pd, Pt) suggest, that (i) the free stannylene **12** is not formed during the reported reactions. This is in agreement with the absence of stannylene dimerization products. (ii) In all considered mechanistic scenarios stannylene complexes **17** are formed in the first step. These metal stannylene complexes (**17**) can undergo a two step isomerization reaction via an intermediate metallostannylene (**20**) to give the silastannene complex **19** with overall barriers which are for each metal of the triad, Ni, Pd, Pt, significantly smaller than the activation energy predicted for the rearrangement of the free stannylene **12** to the cyclic stannasilene **15**. This provides a solid indication that the experimentally observed silyl group migration occurs only after complexation to the metal. (iii) According to the calculations for our model systems, the rearrangement of the nickel-stannylene complex $\mathbf{17a^{Me}}$ is connected with the highest barrier of the metals of the triad. This kinetic factor should be also important for the stability versus the rearrangement of nickel-stannylene complexes such as **11**. In addition, the outcome of our computations revealed, that there is a subtle energetic balance between metal-stannylenes such as **17** and the isomeric silastannene complexes, for example, **19**, which is significantly influenced by steric and/or electronic effects of the substituent at the tin or the metal atom. This is shown in the nickel case by the reversed energetic sequence for the two isomer pairs $\mathbf{17a^{Me}}$/$\mathbf{19a^{Me}}$ (silastannene complex **19** more stable) and **11**/**21** (nickel stannylene complex **11** more stable).

The rearrangement chemistry from the stannylene to the isomeric silastannene complex is remarkable as it is related to the behavior of free silylated tetrylenes, which exhibit this behavior as a means of stabilizing themselves.[4,41] The fact that this reactivity pattern is enhanced in the coordination sphere of a transition metal suggests that similar rearrangement processes might be catalyzed by transition metal complexes.

## 4. EXPERIMENTAL SECTION

**General Remarks.** All reactions involving air-sensitive compounds were carried out under an atmosphere of dry nitrogen or argon using either Schlenk techniques or a glovebox. All solvents were dried using column based solvent purification system.[42] Chemicals were obtained from different suppliers and used without further purification. Phosphine stabilized stannylene **1**,[5] $Sn[N(SiMe_3)_2]_2$,[43] $(Et_3P)_4Pd$,[44] and tris(trimethylsilyl)silylpotassium[17] were prepared following reported procedures.

$^1H$ (300 MHz), $^{13}C$ (75.4 MHz), $^{29}Si$ (59.3 MHz), $^{31}P$ (124.4 MHz), and $^{119}Sn$ (111.8 MHz) NMR spectra were recorded on a Varian INOVA 300 spectrometer. If not noted otherwise for all samples $C_6D_6$ was used or in case of reaction samples, they were measured with a $D_2O$ capillary in order to provide an external lock frequency signal. To compensate for the low isotopic abundance of $^{29}Si$ the INEPT pulse sequence was used for the amplification of the signal.[45,46] Elementary analysis was carried out using a Heraeus VARIO ELEMENTAR.

**X-ray Structure Determination.** For X-ray structure analyses the crystals were mounted onto the tip of glass fibers, and data collection was performed with a BRUKER-AXS SMART APEX CCD diffractometer using graphite-monochromated Mo K$\alpha$ radiation (0.71073 Å). The data were reduced to $F^2_o$ and corrected for absorption effects with SAINT[47] and SADABS,[48,49] respectively. The structures were solved by direct methods and refined by full-matrix least-squares method (SHELXL97).[50] If not noted otherwise all non-hydrogen atoms were refined with anisotropic displacement parameters. All hydrogen atoms were located in calculated positions to correspond to standard bond lengths and angles. Crystallographic data (excluding structure factors) for the structures of compounds **3**, **6**, **7**, **8**, **9**, **10**, and **11** reported in this paper have been deposited with the Cambridge Crystallographic Data Center as supplementary publication no. CCDC-854111 (**3**), 854115 (**6**), 854112 (**7**), 831747 (**8**), 854113 (**9**), 854114 (**10**), and 854116 (**11**). Copies of data can be obtained free of charge at: http://www.ccdc.cam.ac.uk/products/csd/request/.

**Silastannene Platinum Complex 3.** A mixture of **1** (351 mg, 0.5 mmol), $dppePtCl_2$ (332 mg, 0.5 mmol) and potassium (40 mg, 1.0 mmol) was suspended in benzene and stirred for 16 h at rt. The solvent was removed under reduced pressure, and the remaining black solid was extracted with pentane (three times, 5 mL each). The deep red filtrate was concentrated to 5 mL and stored at −60 °C for 24 h. Red crystals of **3** (341 mg, 58%) were isolated by decantation. $^1H$ NMR ($\delta$ in ppm): 7.77 - 6.87 (m, 20H, dppe-phenyl), 1.90 − 1.69 (m, 4H, dppe-$CH_2$), 0.76 (s, 3H, $SiMe_2$), 0.54 (s, 9H, $SiMe_3$), 0.50 (s, 3H, $SiMe_2$), 0.44 (s, 9H, $SiMe_3$), 0.32 (s, 9H, $SiMe_3$), 0.28 (s, 3H, $SiMe_2$), 0.28 (s, 3H, $SiMe_2$), 0.23 (s, 9H, $SiMe_3$). $^{13}C$ NMR ($\delta$ in ppm): 133.4, 133.2, 133.1, 132.3, 129.6, 128.5, 127.3, 127.0, 125.8, 123.9, 28.2−26.9 (m, dppe-bridge), 5.5, 4.6, 3.2, 2.7, 1.5, −0.1, −0.6, −1.7. $^{29}Si$ NMR ($\delta$ in ppm): −6.9, −7.1, −8.1 (dd, $^3J_{SiP}$ = 3.1 Hz, 3.8 Hz), −8.8 (dd, $^3J_{SiP}$ = 0.7 Hz, 2.9 Hz), −13.8 (vt-t, $^3J_{SiP}$ = 2.6 Hz), −22.0, −62.5 (dd, trans-$^2J_{PSi}$ = 99.7 Hz; cis-$^2J_{PSi}$ = 14.0 Hz), −124.8 Hz (d, $^3J_{SiP}$ = 1.1 Hz, $^1J_{SiSn}$ = 12.1). $^{31}P$ NMR ($\delta$ in ppm): 61.1 (d, $^2J_{PP}$ = 10 Hz, $^1J_{PPt}$ = 2415 Hz, *cis*-$^2J_{PSn}$ = 108 Hz), 42.6 (d, $^2J_{PP}$ = 10 Hz, $^1J_{PPt}$ = 2688 Hz, *trans*-$^2J_{PSn}$ = 668 Hz). $^{119}Sn$ NMR ($\delta$ in ppm): −488.0 (dd, *cis*-$^2J_{PSn}$ = 108 Hz, *trans*-$^2J_{PSn}$ = 668 Hz, $^1J_{PtSn}$ = 2990 Hz). Anal. Calcd for $C_{42}H_{72}P_2PtSi_8Sn$ (1177.46): C 42.84, H 6.16. Found: C 42.45, H 5.92.

**Silastannene Palladium Complex 6.** *Method A via Complex 4.* A solution of $(Ph_3P)_4Pd$ (80 mg, 0.07 mmol) in benzene (2 mL) was added dropwise to **1** (49 mg, 0.07 mmol) in benzene (3 mL). After stirring for 1 h at rt the deep red solution was subjected to NMR control and complete conversion to **4** was found. (NMR for **4** measured in benzene, an external lock signal was provided by a $D_2O$ filled capillary. $^{29}Si$ NMR ($\delta$ in ppm): −4.2, −8.3, −8.5, −8.6, −18.5, −20.6, −35.8 (dd, *cis*-$^2J_{PSi}$ = 26.2 Hz, *trans*-$^2J_{PSi}$ = 97.0 Hz), −124.6. $^{31}P$ NMR ($\delta$ in ppm): 23.7 (d, $^2J_{PP}$ = 13.1 Hz, $^2J_{119SnP}$ = 161 Hz, $^2J_{117SnP}$ = 144 Hz), −10.5 (d, $^2J_{PP}$ = 13.1 Hz, $^2J_{SnP}$ = 641 Hz). $^{119}Sn$ NMR ($\delta$ in ppm): −280.3 (dd, *cis*-$^2J_{PSn}$ = 161 Hz, *trans*-$^2J_{PSn}$ = 641 Hz). All attempts to isolate **4** by crystallization failed so dppe (28 mg, 0.07 mmol) solved in pentane was added. After stirring for 1 h at rt the solvent was removed under reduced pressure. Crystallization with pentane at −60 °C gave after 48 h pure **6** (37 mg, 48%).

*Method B via Complex 5.* A solution of $(Et_3P)_4Pd$ (83 mg, 0.14 mmol) in pentane (2 mL) was added dropwise to **1** (100 mg, 0.14 mmol) in pentane (3 mL). After stirring for 1 h at rt the deep red solution was subjected to NMR control and complete conversion to **5** was found. (NMR for **5** measured in pentane, an external lock signal was provided by a $D_2O$ filled capillary.) $^{29}Si$ NMR ($\delta$ in ppm): −3.8 (dd, *cis*-$^3J_{SiP}$ = 6.9 Hz; *trans*-$^2J_{SiP}$ = 8.7 Hz), −5.9 (vt-t: $^3J_{PSi}$ = 4.2 Hz), −8.5, −8.7, −18.6 (vt-t, $^3J_{SiP}$ = 4.4 Hz), −22.1, −42.2 (dd, *cis*-$^2J_{SiP}$ = 26.3 Hz, *trans*-$^2J_{PSi}$ = 101.8 Hz), −126.3. $^{31}P$ NMR ($\delta$ in ppm): 10.7 (d, $^2J_{PP}$ = 14.5 Hz, $^2J_{SnP}$ = 161 Hz), −5.2 (d, $^2J_{PP}$ = 14.5 Hz, $^2J_{SnP}$ = 656 Hz). $^{119}Sn$ NMR ($\delta$ in ppm): −310.2 (dd, *cis*-$^2J_{SnP}$ = 161 Hz, *trans*-$^2J_{SnP}$ = 656 Hz). Again all attempts to isolate **5** by crystallization failed so dppe (56 mg, 0.14 mmol) solved in pentane was added. After stirring for 1 h at rt the solvent was removed under reduced pressure. Crystallization with pentane at −60 °C gave after 72 h pure **6** (98 mg, 64%).

*Method C.* **1** (100 mg, 0.14 mmol), $dppePdCl_2$ (82 mg, 0.14 mmol) and potassium (11 mg, 0.28 mmol) were suspended in 5 mL benzene, sonificated for 5 min and then stirred for 24 h at rt. The solvent was removed under reduced pressure, and the remaining black solid was extracted with pentane (three times, 4 mL each). The deep red filtrate was concentrated to 3 mL and stored at −60 °C for 36 h. Red crystals

of **6** (84 mg, 56%) could be isolated by decantation. $^{1}$H NMR ($\delta$ in ppm): 6.90 − 7.80 (m, 20H), 1.91 − 1.60 (m, 4H, dppe-$CH_2$), 0.51 (s, 3H), 0.49 (s, 9H), 0.45(s, 3H), 0.43 (s, 3H), 0.34 (s, 9H), 0.29 (s, 9H), 0.26 (s, 3H), 0.15 (s, 9H). $^{13}$C NMR ($\delta$ in ppm): 133.9, 133.7, 133.2, 133.0, 132.4, 132.3, 128.4, 28.1 − 26.4 (m, $CH_2$-dppe), 4.6, 4.3, 3.3, 2.8, 1.0, −0.5, −1.4, −2.8. $^{29}$Si NMR ($\delta$ in ppm): −2.1, −3.6 (dd, $^{3}J_{PSi}$ = 4.0 Hz, $^{3}J_{PSi}$ = 10.9 Hz), −6.5, −8.6, −15.5 (vt-t, $^{3}J_{PSi}$ = 4.1 Hz), −22.9, −30.8 (dd, *cis*-$^{2}J_{SiP}$ = 17.9 Hz, *trans*-$^{2}J_{SiP}$ = 91.1 Hz), 121.8 (d, $^{3}J_{SiP}$ = 2,0 Hz). $^{31}$P NMR ($\delta$ in ppm): 40.4 (d, $^{2}J_{PP}$ = 13.1 Hz, $^{2}J_{PSn}$ = 100.5 Hz), 23.5 (dd, $^{2}J_{PP}$ = 13.1 Hz, $^{2}J_{PSn}$ = 546 Hz). $^{119}$Sn NMR ($\delta$ in ppm): −316.3 (dd, *cis*-$^{2}J_{SnP}$ = 113 Hz, *trans*-$^{2}J_{SnP}$ = 560 Hz). Anal. Calcd for $C_{42}H_{72}P_2PdSi_8Sn$ (1088.80): C 46.33, H 6.67. Found: C 45.84, H 6.89.

**Stannide Complex 7.** Freshly prepared tris(trimethylsilyl)-silylpotassium [starting with tetrakis(trimethylsilyl)silane (642 mg, 2.0 mmol) and KO*t*Bu (236 mg, 2.1 mmol) in 4 mL THF] in pentane (5 mL) was added to a solution of $Sn[N(SiMe_3)_2]_2$ in pentane (5 mL) at −90 °C. The reaction mixture was allowed to warm up to rt and during this time the color changed from green to red. After filtration and concentration to 4 mL the solution was stored at −60 °C for 72 h. Red crystals of **7** (671 mg, 70%) could be isolated by decantation. $^{1}$H NMR ($\delta$ in ppm): 3.41 (m, 8H, THF), 1.38 (m, 8H, THF), 0.56 (s, 18H, $N(SiMe_3)_2$), 0.15 (s, 54H). $^{13}$C NMR ($\delta$ in ppm): 67.9 (THF), 24.9 (THF), 6.5, 5.6 ($N(SiMe_3)_2$). $^{29}$Si NMR ($\delta$ in ppm): −6.6, −20.4 ($N(SiMe_3)_2$), −127.6. $^{119}$Sn NMR ($\delta$ in ppm): 96.1.

**$SnCl_2$−$PEt_3$ Adduct 8.** $SnCl_2$ (180 mg, 1.0 mmol) was suspended in THF (ca. 2 mL) and stirred at rt. A solution of $PEt_3$ (120 mg, 1.0 mmol) in THF (ca. 1 mL) was added and stirring was continued for 30 min until a clear solution had developed. Some drops of pentane were added and the resulting slightly cloudy suspension was centrifuged. The resulting clear colorless solution was stored at −60 °C for 72 h. Colorless big needle shaped crystals of **8** (302 mg, 98%) were isolated by decantation and dried in vacuo. NMR spectra of **8** were recorded in THF, an external lock signal was provided by a $D_2O$ filled capillary. $^{1}$H NMR ($\delta$ in ppm): 1.87 (br, 6H, $P(CH_2CH_3)_3$), 1.16 (br, 9H, $P(CH_2CH_3)_3$). $^{13}$C NMR ($\delta$ in ppm): 14.1 ($P(CH_2CH_3)_3$), 7.7 ($P(CH_2CH_3)_3$). $^{31}$P NMR ($\delta$ in ppm): −3.7 (br). $^{119}$Sn NMR ($\delta$ in ppm): −82.5 (br). Anal. Calcd for $C_6H_{15}Cl_2PSn$ (307.77): C 23.41, H 4.91. Found: C 23.49, H 4.99.

**Bis[tris(trimethylsilyl)silyl]stannylene Triethylphosphine Adduct 9.** Freshly prepared tris(trimethylsilyl)silylpotassium (starting with same amount as for **7**) was added to **8** (308 mg, 1.00 mmol) in THF (3 mL). The red suspension was stirred for 3 h at rt. The solvent was removed under reduced pressure, and the remaining black solid was extracted with pentane (three times, 4 mL each). After concentration to 4 mL the solution was stored at −60 °C for 36 h. Red crystals of **9** (564 mg, 77%) could be isolated by decantation. $^{1}$H NMR ($\delta$ in ppm): 1.59 (dq, $^{3}J_{HH}$ = 7.2 Hz, $^{2}J_{PH}$ = 7.0 Hz, 6H, $P(CH_2CH_3)_3$), 0.83 (dt, $^{3}J_{HH}$ = 7.2 Hz, $^{3}J_{PH}$ = 14.4 Hz, 9H, $P(CH_2CH_3)_3$), 0.44 (s, 54H, $SiMe_3$). $^{13}$C NMR ($\delta$ in ppm): 18.9 (d, $^{2}J_{PC}$ = 9 Hz, $P(CH_2CH_3)_3$), 8.9 ($P(CH_2CH_3)_3$), 5.3 ($SiMe_3$). $^{29}$Si NMR ($\delta$ in ppm): −7.0, −127.6. $^{31}$P NMR ($\delta$ in ppm): −17.4 (br). $^{119}$Sn NMR ($\delta$ in ppm): −113.3 (br).

**Silastannene Palladium Complex 10.** **9** (366 mg, 0.5 mmol), $dppePdCl_2$ (288 mg, 0.5 mmol) and potassium (40 mg, 1.0 mmol) were suspended in toluene and stirred for 16 h at rt. The solvent was removed under reduced pressure, and the remaining black solid was extracted with pentane (three times, 4 mL each). The deep red filtrate was concentrated to 5 mL and stored at −60 °C for 36 h. Red crystals of **10** (353 mg, 63%) could be isolated by decantation. $^{1}$H NMR ($\delta$ in ppm): 7.03 − 7.55 (m, 20H), 1.93 − 1.62 (m, 4H, dppe-$C_2H_4$), 0.48 (s, 9H), 0.40 (s, 9H), 0.38 (s, 27H), 0.36 (s, 9H). $^{13}$C NMR ($\delta$ in ppm): 133.9, 133.7, 133.5, 133.4, 132.8, 132.7, 129.9, 129.7, 129.2, 28.4 − 27.1 (m, dppe-$C_2H_4$), 7.3, 5.9, 5.4, 4.3. $^{29}$Si NMR ($\delta$ in ppm): −4.2, −5.5, −9.2, −9.8, −40.8 (dd, *cis*-$^{2}J_{PSi}$ = 16 Hz, *trans*-$^{2}J_{PSi}$ = 89 Hz), −121.9. $^{31}$P NMR ($\delta$ in ppm): 40.8 (d, $^{2}J_{PP}$ = 9.4 Hz, $^{2}J_{119/117SnP}$ = 108 Hz, 124 Hz), 26.0 (d, $^{2}J_{PP}$ = 9.4 Hz, $^{2}J_{117/119SnP}$ = 612 Hz, 635 Hz). $^{119}$Sn NMR ($\delta$ in ppm): −430.2 (dd, *cis*-$^{2}J_{SnP}$ = 89 Hz, *trans*-$^{2}J_{PSn}$ = 635 Hz). Anal. Calcd for $C_{44}H_{78}P_2PdSi_8Sn$ (1118.87): C 47.23, H 7.03. Found: C 47.50, H 6.96.

**Nickel Stannylene Complex 11.** $Ni(COD)_2$ (30 mg, 0.11 mmol) and **9** (80 mg, 0.11 mmol) were suspended in benzene (4 mL) and stirred for 1 h at rt. $PEt_3$ (13 mg, 0,11 mmol) was added and the stirring continued for another 30 min. The solvent was removed under reduced pressure, and the remaining red solid was solved with pentane (3 mL). After 72 h at −60 °C violet crystals of **11** (30 mg, 43%) were isolated by decantation. $^{1}$H NMR ($\delta$ in ppm): 1.30 (m, 18H, $P(CH_2CH_3)_3$), 0.92 (dq, $^{3}J_{HH}$ = 7.2 Hz, $^{2}J_{PH}$ = 13.3 Hz, 12H, $P(CH_2CH_3)_3$), 0.37 (s, 54H). $^{13}$C NMR ($\delta$ in ppm): 19.1 ($P(CH_2CH_3)_3$), 7.8 ($P(CH_2CH_3)_3$), 2.8 ($SiMe_3$). $^{29}$Si NMR ($\delta$ in ppm): −10.1 (t, $^{3}J_{PSi}$ = 3.2 Hz), −94.0 (t, $^{4}J_{PSi}$ = 1.6 Hz). $^{31}$P NMR ($\delta$ in ppm): 25.7 ($^{2}J_{SnP}$ = 611 Hz). $^{119}$Sn NMR ($\delta$ in ppm): 1314.4 (t, $^{2}J_{SnP}$ = 611 Hz). Anal. Calcd for $C_{30}H_{84}NiP_2Si_8Sn$ (909.03): C 39.64, H 9.31. Found: C 39.57, H 9.42.

## ■ ASSOCIATED CONTENT

### Supporting Information

Crystallographic information for compounds **3**, and **6**−**11** in CIF format. Technical details of the computations, calculated structures of compounds **5**−**13**, **15**, **19**−**21**, and some additional reference compounds (**22**−**33**). Complete reference 32. This material is available free of charge via the Internet at http://pubs.acs.org.

## ■ AUTHOR INFORMATION


### Corresponding Author

christoph.marschner@tugraz.at; baumgartner@tugraz.at; thomas.mueller@uni-oldenburg.de


### Notes

The authors declare no competing financial interest.

## ■ ACKNOWLEDGMENTS


Support for this study was provided by the Austrian *Fonds zur Förderung der wissenschaftlichen Forschung* (FWF) via the projects P-19338 (C.M.), P-21346 (J.B.), and P-25124 (J.B.). P.Z. thanks the *Fonds der Chemischen Industrie* (FCI) for a scholarship (No.183191). The High-End Computing Resource Oldenburg (HERO) at the CvO University is thanked for computer time.


## ■ REFERENCES


(1) Mizuhata, Y.; Sasamori, T.; Tokitoh, N. *Chem. Rev.* **2009**, *109*, 3479−3511.

(2) Klinkhammer, K. W.; Schwarz, W. *Angew. Chem., Int. Ed. Engl.* **1995**, *34*, 1334−1336.

(3) Klinkhammer, K. *Polyhedron.* **2002**, *21*, 587−598.

(4) Hlina, J.; Baumgartner, J.; Marschner, C.; Albers, L.; Müller, T. *Organometallics* **2013**, accepted.

(5) Arp, H.; Baumgartner, J.; Marschner, C.; Müller, T. *J. Am. Chem. Soc.* **2011**, *133*, 5632−5635.

(6) Arp, H.; Baumgartner, J.; Marschner, C.; Zark, P.; Müller, T. *J. Am. Chem. Soc.* **2012**, *134*, 6409−6415.

(7) Arp, H.; Baumgartner, J.; Marschner, C.; Zark, P.; Müller, T. *J. Am. Chem. Soc.* **2012**, *134*, 10864−10875.

(8) Krause, J.; Pluta, C.; Pörschke, K.-R.; Goddard, R. *J. Chem. Soc., Chem. Commun.* **1993**, 1254−1256.

(9) Pluta, C.; Pörschke, K. R.; Mynott, R.; Betz, P.; Krüger, C. *Chem. Ber.* **1991**, *124*, 1321−1325.

(10) Sharma, H. K.; Pannell, K. H. *Chem. Rev.* **1995**, *95*, 1351−1374.

(11) Okazaki, M.; Tobita, H.; Ogino, H. *Dalton Trans.* **2002**, 493−506.

(12) Ogino, H. *Chem. Rec.* **2002**, *2*, 291−306.

(13) Zirngast, M.; Marschner, C.; Baumgartner, J. *Organometallics* **2006**, *25*, 4897−4908.

(14) Katir, N.; Matioszek, D.; Ladeira, S.; Escudié, J.; Castel, A. *Angew. Chem., Int. Ed.* **2011**, *50*, 5352−5355.

(15) Klinkhammer, K. W.; Schwarz, W. *Z. Anorg. Allg. Chem.* **1993**, *619*, 1777−1789.
(16) Niemeyer, M. In *Organosilicon Chemistry IV: From Molecules to Materials*; Auner, N., Weis, J., Eds.; Wiley-VCH: New York, 2005; Vol. *1*, pp 323−329.
(17) Marschner, C. *Eur. J. Inorg. Chem.* **1998**, 221−226.
(18) Du Mont, W.-W.; Neudert, B.; Schumann, H. *Angew. Chem., Int. Ed.* **2003**, *15*, 308−309.
(19) Bogdanović, B.; Kröner, M.; Wilke, G. *Liebigs Ann. Chem.* **1966**, *699*, 1−23.
(20) Watanabe, C.; Inagawa, Y.; Iwamoto, T.; Kira, M. *Dalton Trans.* **2010**, *39*, 9414−9420.
(21) Tanabe, M.; Hanzawa, M.; Osakada, K. *Organometallics* **2010**, *29*, 3535−3540.
(22) Kira, M.; Sekiguchi, Y.; Iwamoto, T.; Kabuto, C. *J. Am. Chem. Soc.* **2004**, *126*, 12778−12779.
(23) Hashimoto, H.; Sekiguchi, Y.; Iwamoto, T.; Kabuto, C.; Kira, M. *Organometallics* **2002**, *21*, 454−456.
(24) Hashimoto, H.; Sekiguchi, Y.; Sekiguchi, Y.; Iwamoto, T.; Kabuto, C.; Kira, M. *Can. J. Chem.* **2003**, *81*, 1241−1245.
(25) Iwamoto, T.; Sekiguchi, Y.; Yoshida, N.; Kabuto, C.; Kira, M. *Dalton Trans.* **2006**, 177−182.
(26) Al-Allaf, T. A. K. *J. Organomet. Chem.* **1999**, *590*, 25−35.
(27) Al-Allaf, T. A. K. *J. Organomet. Chem.* **2002**, *654*, 21−28.
(28) Sekiguchi, A.; Izumi, R.; Lee, V. Y.; Ichinohe, M. *J. Am. Chem. Soc.* **2002**, *124*, 14822−14823.
(29) Mackay, K. M. In *The Chemistry of Organic Germanium, Tin and Lead Compounds*; Patai, S., Ed.; John Wiley & Sons: New York, 1995; Vol. *1*, pp 97−194.
(30) Becker, M.; Foerster, C.; Franzen, C.; Hartrath, J.; Kirsten, E.; Knuth, J.; Klinkhammer, K. W.; Sharma, A.; Hinderberger, D. *Inorg. Chem.* **2008**, *47*, 9965−9978.
(31) The pyramidalization angle $\beta$ is defined as the angle between the vector of the exocyclic E−Sn bond and the plane spanned by the Sn atom and the two adjacent Si atoms.
(32) The Gaussian 09 program was used. Frisch, M. J.; et al. *Gaussian 09*, Revision B.01; Gaussian, Inc.: Wallingford, CT, 2010. For detailed description of the computations, see the Supporting Information.
(33) Jutzi, P.; Leue, C. *Organometallics* **1994**, *13*, 2898−2899.
(34) Eichler, B. E.; Phillips, A. D.; Haubrich, S. T.; Mork, B. V.; Power, P. P. *Organometallics* **2002**, *21*, 5622−5627.
(35) Pu, L.; Power, P. P.; Boltes, I.; Herbst-Irmer, R. *Organometallics* **2000**, *19*, 352−356.
(36) Pu, L.; Twamley, B.; Haubrich, S. T.; Olmstead, M. M.; Mork, B. V.; Simons, R. S.; Power, P. P. *J. Am. Chem. Soc.* **2000**, *122*, 650−656.
(37) Hayes, P. G.; Gribble, C. W.; Waterman, R.; Tilley, T. D. *J. Am. Chem. Soc.* **2009**, *131*, 4606−4607.
(38) Pandey, K. K.; Lein, M.; Frenking, G. *J. Am. Chem. Soc.* **2003**, *125*, 1660−1668.
(39) Pandey, K. K.; Lledós, A. *Inorg. Chem.* **2009**, *48*, 2748−2759.
(40) Pandey, K. K.; Power, P. P. *Organometallics* **2011**, *30*, 3353−3361.
(41) Xiao, X.-Q.; Zhao, H.; Xu, Z.; Lai, G.; He, X.-L.; Li, Z. *Chem. Commun.* **2013**, *49*, 2706−2708.
(42) Pangborn, A. B.; Giardello, M. A.; Grubbs, R. H.; Rosen, R. K.; Timmers, F. J. *Organometallics* **1996**, *15*, 1518−1520.
(43) Schaeffer, C. D.; Myers, L. K.; Coley, S. M.; Otter, J. C.; Yoder, C. H. *J. Chem. Educ.* **1990**, *67*, 347−349.
(44) Schunn, R. A. *Inorg. Chem.* **1976**, *15*, 208−212.
(45) Morris, G. A.; Freeman, R. *J. Am. Chem. Soc.* **1979**, *101*, 760−762.
(46) Helmer, B. J.; West, R. *Organometallics* **1982**, *1*, 877−879.
(47) *SAINTPLUS: Software Reference Manual*, Version 6.45; Bruker-AXS: Madison, WI, 1997−2003.
(48) Blessing, R. H. *Acta Cryst. A.* **1995**, *51*, 33−38.
(49) Sheldrick, G. M. *SADABS*, Version 2.10; Bruker AXS Inc.: Madison, WI, 2003.
(50) Sheldrick, G. M. *Acta Cryst. A* **2007**, *64*, 112−122.